Journal of the European Ceramic Society 19 (1999) 1935–1948

PII: S0955-2219(99)00007-2
0955-2219/99/$ - see front matter

Influence of the Temperature on the Stability of Aqueous Alumina Suspensions

Cécile Pagnoux,* Marina Serantoni, Richard Laucournet, Thierry Chartier and Jean-François Baumard

ESA CNRS 6015, 87065 Limoges cedex, France

(Received 12 October 1998; accepted 30 December 1998)

Abstract

Ceramic process need the preparation of very stable suspensions with high solid loading and the temperature is a fundamental parameter in surface chemistry and at various steps in the production process. The influence of the temperature on the stability of aqueous alumina suspensions dispersed either with the polymethacrylic acid sodium salt either with the Tiron has been studied. The strong adsorption of the two dispersants onto alumina surface is not affected by the variation of the temperature but temperature higher than 40°C strongly influences the amplitude of the repulsive potential created between the particules. By using the potentimetric data fitting software FITEQL 3·2, the electrokinetic properties of the suspensions at 20°C are interpreted and viscosity measurements show that a temperature of 60°C improves the stability of the suspensions and permits to concentrate it. © *1999 Elsevier Science Limited. All rights reserved*

Keywords: suspensions, electrokinetic properties, surfaces, Al_2O_3, temperature.

1 Introduction

For many applications in ceramic processing, highly concentrated ceramic suspensions are required to lead to high performance final products. Well known parameters such as particle size, solid loading, pH and ionic strength affect the characteristics of the slurries but the stability of the colloidal suspensions can be greatly improved by adding dispersants. In aqueous media, organic compounds as polyelectrolytes are widely used because both steric and electrostatic mechanisms can contribute to the stability of the suspensions.[1,2]

Several works[3–5] have been dedicated to the influence of the pH and of the ionic strength on the adsorption of the polymer onto the particle surface. Electrostatic interactions between the particle surface and the dispersant are driving the adsorption. These interactions results from the ionisation of the polymer and from the polarity of the surface charge of the particles, which depend itself in particular on the pH. Baklouti *et al.*[6] related the chemistry of the particles surface and of the polymer to the mechanism of the powder dispersion and used this approach to disperse αSiC powder in water.

In water a high repulsive potential then a high stability can be created by using a electrolyte.[7] On one hand, the ability of some of these electrolytes to form chelate rings with ions of the particle surface leads to a strong adsorption and on a second hand, the ionised groups develop a surface charge which induces a high repulsive potential. Some work on ceramic processes such as the direct coagulation casting (DCC)[7] has been carried out with an ammonium salt of citrate used as defloculant for alumina powder in aqueous media. The influence of the chemical structure of this type of molecule onto the stability of alumina suspensions has been studied by Pirmin *et al.*[8]

All these studies contributed to a better understanding of the chemistry of surface and of the interactions with dispersant molecules but few concern the influence of the temperature on the stability of ceramic suspensions.[9] Nevertheless it is a fundamental parameter in surface chemistry and at various steps in the production process. Significant temperature variations may arise and can change the characteristics of the slurry for example, during milling and during the critical stage of drying which can lead to cracking of the green bodies and which may be better controlled with the variation of the temperature. The temperature influences a lot of parameters in chemistry surface

*To whom correspondence should be addressed.

such as pH, viscosity of the solvent, chemistry of organic additives or the surface potentials expressed in the theoretical models.

The aim of this study is to determine the influence of the temperature on the adsorption and the electrokinetic behaviour of aqueous alumina suspensions dispersed either with a polyelectrolyte, the polymethacrylic acid sodium salt (PMAANa) and or with an electrolyte, the 4,5-dihydroxy-1,3-benzenedisulfonic acid sodium salt monohydrate, Tiron. The triple layer model (TLM) was used to model the variations of the zeta potential of alumina suspension at 20°C versus pH. Finally, the electrokinetic properties of alumina suspensions at 20°C are interpreted and some hypothesis concerning the influence of the temperature onto these properties are given using a potentiometric data fitting software FITEQL 3·2.[10]

2 Experimental Procedure

2.1 Starting materials

The main features of the alumina powders used in this study are summarized in Table 1.

The dispersants used were the 4,5-dihydroxy-1,3-benzenedisulfonic acid sodium salt monohydrate, Tiron (Aldrich) and the polymethacrylic acid sodium salt (PMAANa), 30 wt% solution in water, with an average molecular weight of 9500 (GPC) (Aldrich). The water used in all experiments was bidistilled.

The titrations of PMAANa and the adjustment of the pH values of the suspensions were carried out with solutions of standard analytical-grade, NaOH and HCl [normadose™ 1 mol l^{-1} (±0·5%), Prolabo, Germany]. Analytical grade NaCl used for adjusting the ionic strength was supplied by Aldrich.

2.2 Preparation of the Suspensions

In order to obtain the chemical equilibrium of the slurries for adsorption, viscosity and ESA measurements, the alumina powder was previously deagglomerated in water with the dispersant by ultrasonic treatment (pulsed, 3 min, 600 W, Vibra-cell ultrasonic desintegrator VC 600, Sonic & Materials, USA). To avoid overheating during this treatment, the flask containing the suspension is placed in a glass-bath.

Table 1. Powders used in the present work

Reference—purity —supplier	*Specific surface area N_2 BET 2 h at 300°C (m^2 g^{-1})*	*Average grain size (μm) Sedigraph 5100 Micrometrics*
A16SG > 99·8% Alcoa Pittsburgh USA	9	0·5
AKP30 > 99·99% Sumitomo Japan	10	0·4

Then, the suspensions were stirred for 12 h at a fixed temperature by using a thermostatic bath. The amount of dispersant added into the suspension was expressed as a percentage of the alumina dry weight.

Adsorption Slurries were prepared with 60 wt% solid (A16SG) loading with different amounts of dispersant at a temperature of 10, 20, 40 and 60°C. After 12 h, suspensions were centrifuged at high speed during 5 mn, then the supernatant removed and analysed. The amount of dispersant adsorbed onto the surface of the powder was calculated from the difference between the amount added and that remaining in the supernatant. We considered that the short time of centrifugation at room temperature did not influence the quantity of dispersant adsorbed.

As Tiron is a sulphonic acid, then the sulphur content in the supernatant was determined by chemical analysis and then the Tiron concentration calculated.

The quantity of PMAANa was determined by acidic titration.[11] Ten millilitres of supernatant was taken from every sample and diluted with 90 ml of water. The ionic strength was adjusted to obtain a solution of 10^{-2} mol l^{-1} of NaCl and the pH at 10 to ensure that any PMAANa would be fully dissociated. The titrations, carried out in N_2-flux were made with the HCl 0·5 M solution as titrant using the automatic titration unit which equips the acoustosizer (ESA 8000 MATEC) and can deliver a minimum volume of titrant equal to 1 μl.

Standard solutions were prepared in the same conditions (ionic strength and pH) to establish the linear relationship between the amount of PMAANa titrated and the mole equivalent of titrant. Titration curves showed two inflexion points (Fig. 1), the first corresponds to NaOH which had not dissociated the polyelectrolyte and then in excess. The volume of titrant measured between the two inflexion points corresponds to the quantity of PMAANa contained in the standard solution. The calibration results were fitted to a straight line using linear regression.

Furthermore the supernatant of an A16SG alumina suspension (60 wt%) without defloculant was titrated and the curve showed also two inflexion points. The first corresponds to NaOH which is due to the impurities of the A16SG powder and the second takes place at the same pH than the polyelectrolyte and could be attributed to a weak acid coming from the reaction of the powder in water. This hypothesis seems to be realistic because the curve relative to a supernatant of a pure AKP30 alumina suspension shows only one inflexion point which takes place at the same pH than the second observed for the A16SG supernatant. This second equivalent volume was function of the temperature.

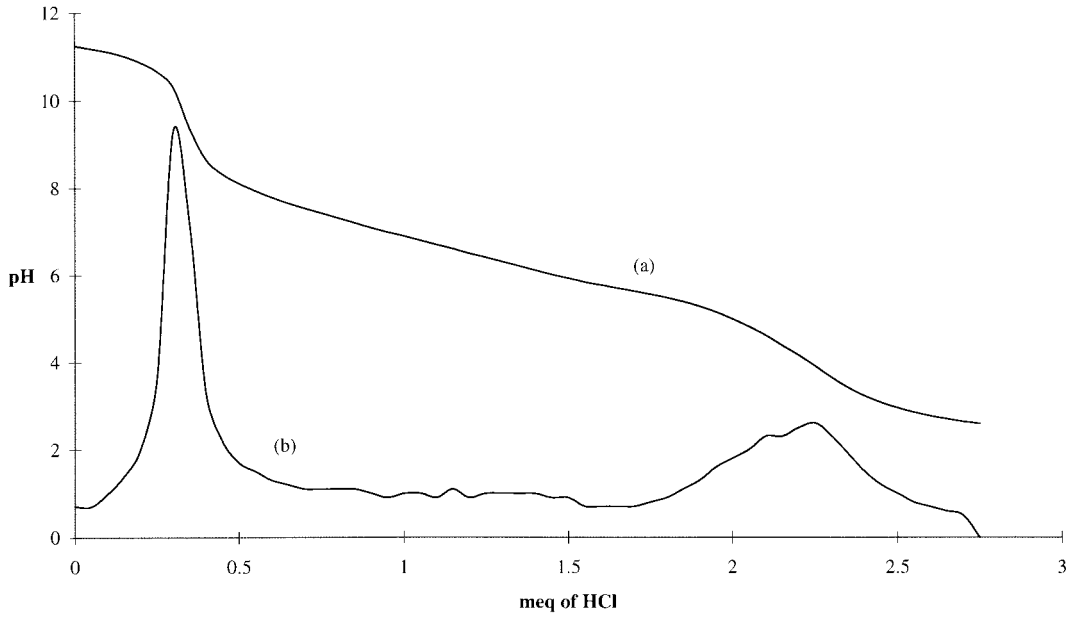

Fig. 1. (a) Titration curve of 0·4 g of PMAANa commercial solution by HCl and (b) its corresponding first derivative plot.

Then for each temperature tested, a blank solution was prepared in the same conditions (pH and ionic strength) than supernatants and the amount of HCl necessary to titrate the weak acid was removed from the volume of HCl measured for each supernatant which was used to establish the adsorption isotherms.

3 Zeta Potential

Electrokinetic measurements provide information on the magnitude of the electrostatic forces of repulsion between ceramic particles. Zeta potential values of the alumina particles in the suspensions were measured using an Electrokinetic Sonic Amplitude (ESA) measurement apparatus (Model ESA8000 Matec, Northborough, MA, USA). This technique and its operating principle were described previously.[12] The experiment consisted in following the evolution of the zeta potential of suspensions prepared with or without dispersant versus pH at 10, 20 and 40°C. Between each incremental addition, the volume delivered is determined automatically by the apparatus, 10 s were allowed for equilibration. During all the experiments, the temperature of the suspension was thermoregulated. The ESA equipment was not able to operate at temperature higher than 40°C without damaging.

The zeta potential was calculated from the magnitude of the ESA signal by using the O'Brien formula[13] but a lot of water characteristics depends on the temperature, namely the velocity of sound, the density of water, the dielectric permittivity, the kinematic viscosity and the viscosity. The relationship between these parameters and the temperature have been established from data of literature and then correct values were used to calculate the zeta potential.

Concerning the measure of pH, a temperature correction must be made when the sample temperature was different from the pH standardization temperature (i.e. 25°C). The temperature correction corresponds to a modification of the slope of the tension (mV) versus pH curve for the pH electrodes with the following equation:

$$\mathrm{pH} = \mathrm{pH_i} - (T_1/T_2)(\mathrm{pH_i} - \mathrm{pH_0}) \qquad (1)$$

where pH is the correct sample pH, $\mathrm{pH_0}$, the pH observed before the correction was applied, $\mathrm{pH_i}$, the isopotential point of the pH electrodes, T_1, the standardization temperature (298 K) and T_2, the sample temperature (K).

4 Results and Discussion

4.1 Adsorption

Figure 2 shows adsorption curves of the two tested molecules on Al_2O_3 (A16SG) particles for different temperatures.

The adsorption curves relative to the Tiron [Fig. 2(a)] show that the quantity chemisorbed increases with the initial amount added whatever the temperature. Furthermore, the amount of Tiron adsorbed between 10 and 60°C slightly increases with the amount of dispersant added (i.e. about 0·02 mg m^{-2} between 0·1 and 0·3 wt% dispersant and 0·05 mg m^{-2} between 0·4 to 0·6 wt%). Tiron chemisorbed in a larger quantity at 60°C.

For an initial addition of 0·15 wt%, all the Tiron was adsorbed, then this molecule should be strongly

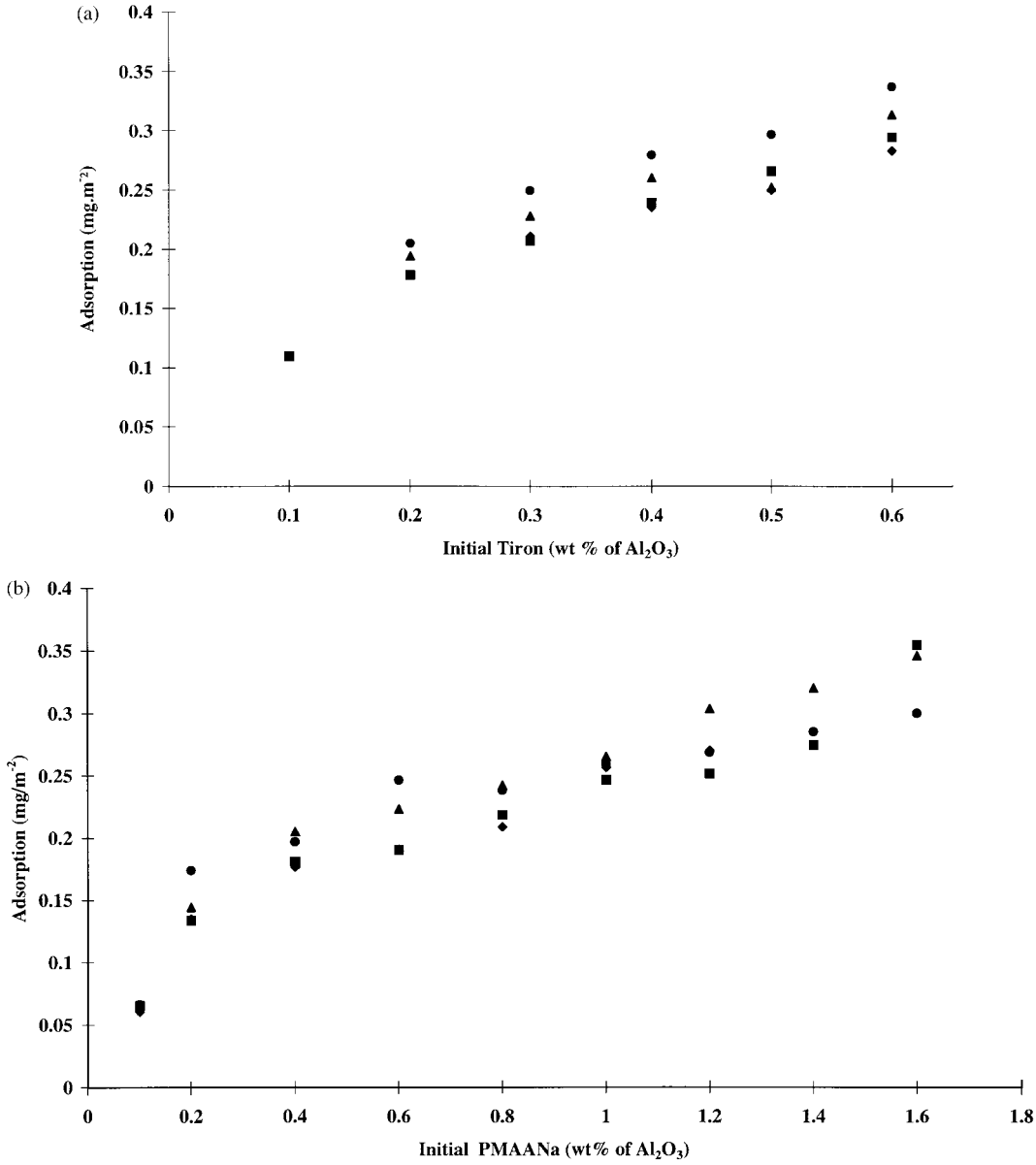

Fig. 2. Adsorption isotherms of (a) Tiron and (b) PMAANa at (◆) 10°C, (■) 20°C, (▲) 40°C and (●) 60°C.

adsorbed onto the particle surface but no well defined plateau is observed on the isotherms. The affinity for the alumina surface of such a molecule with two sulfonate groups ionised in a very large range of pH and which confer to the dispersant a negative charge should depend on the polarity of the surface charge of alumina. Its adsorption can be explained considering the ligand (L)-exchange model, a process involving the following multi-step reaction sequence:[14]

$$LH_{(aq)} \rightarrow L^-_{(aq)} + H^+_{(aq)}$$
$$AlOH_{(s)} + H^+_{(aq)} \rightarrow AlOH^+_2(s)$$
$$AlOH^+_2(s) + L^-_{(aq)} \rightarrow AlL_{(s)} + H_2O$$

In the case of a high concentration of protonated hydroxyl groups at the surface of ceramic particles, which occurs for acidic pH when the hydronium ions adsorbed protonate them, the exchange between the hydroxyl surface groups and the deprotonated ligand easily occurs and leads to a higher affinity of the molecule for the surface.

No control of the pH of the suspensions was performed either in function of the percentage of Tiron either in function of the temperature. Nevertheless, Tiron is a weak acid and should likely decrease the pH of aqueous alumina slurries which is about 9 when no Tiron is added. Furthermore, considering the suspensions (0·2 wt% of Tiron) used for the zeta potential experiments, the value of the starting pH at 10°C is 9·2 and reaches a value of 8·5 at 40°C. In our system, the increase of the initial amounts of Tiron and of the temperature both decrease the pH of the alumina suspensions and then should influence the amount of

Tiron chemisorbed. For each curve, the increase of the quantity chemisorbed with the initial amount introduced could be explained by a higher affinity of the Tiron for the alumina surface with the decrease of pH.

The same tendency can be observed concerning the adsorption of PMAANa on A16SG [Fig. 2(b)] alumina but the increase of the quantity adsorbed with the initial amount introduced is much slower than for Tiron. At 20°C, 0·4 wt% of PMAANa introduced leads to 0·2 mg m^{-2} adsorbed onto the A16SG alumina surface, which is in agreement with values reported in Ref. 11 and the temperature has no significant effect on the quantity adsorbed. At low temperature, the surface of the alumina powder should be almost totally covered by the polyelectrolyte producing the electrosteric stabilisation of the suspension.

Previous studies[6] showed that a high adsorption of polyelectrolytes results from interactions between the ionised groups developed on the polymers and active sites at the oxide surface. By analogy with the Tiron, a decrease of the pH of the suspensions should be favourable for the adsorption of PMAANa.

For these two dispersants, these results show that for an amount of 0·2 and 0·4 wt% of Tiron and PMAANa respectively, the temperature does not influence the quantity adsorbed. The strong adsorption of the Tiron and the PMAANa at low temperature (i.e. 10°C) is not affected at higher temperature (i.e. 60°C).

4.2 Zeta potential

The evolution of the zeta potential versus pH at 10, 20, 40°C was studied for suspensions (AKP30 and A16SG) prepared with and without dispersant. Each slurry was prepared containing a 3·5 vol% solid loading and the ionic strength was adjusted with NaCl. As the temperature influences a lot of physical and chemical parameters relative to the solvent and the solubility of impurities, experiments were performed with a high purity alumina (AKP30) in order to complete these obtained with the A16SG alumina. For the study without dispersant, two suspensions were prepared to obtain the curve in the total range of pH; one from the starting pH to pH 2 and the second from the starting pH to pH 12.

4.3 Without dispersant

The variations of the zeta potential versus pH for the 3 temperatures, 10, 20, 40°C are given in Fig. 3 and the main values used to analyse the data are summarized in the Table 2(a) and (b). Ionic strength was adjusted with 0·01 M NaCl and was considered constant between pH 2·5 and 12.

4.3.1 Effect of pH at 20°C

In a first time, the analysis is focused on the high purity AKP30 powder at 20°C [Fig. 3(a)]. The curve can be divided in three steps. From the smaller negative value of potential (−40 mV) at basic pH (11.5) up to pH 7, the zeta potential increases linearly and is equal to zero at pH 9. Then, in the range of pH from 7 to 5, the zeta potential is constant with a value equal to +25 mV. Finally from pH 5, to the acidic pH 2, the potential increases again to a maximal value of +58 mV.

4.3.1.1. The triple layer model (TLM). In order to understand the mechanisms which govern these three steps, a theoretical model was used to fit experimental data. The model chosen was the single site triple layer model (TLM)[15] which is the one of the most complete model used for describing the surface chemical reactions of oxide minerals in aqueous media. Adsorption is assumed to occur at specific sites on the mineral surface. All sites are considered to be energetically equivalent. These surface sites can also interact with solution constituents such as electrolyte ions or organic molecules. In the three plane model, three electrostatic planes are present, enclosing two empty layers in terms of charge, each with its own electrostatic capacitance. The Stern layer region is divided into two layers, H^+ and OH^- ions contribute to the charge σ_0 and determine the potential Ψ_0. Ions of electrolyte which bind pairwise with oppositely charged surface groups are located at the IHP and are separate from the surface by a region of constant capacity C_1. These ions contribute to the charge σ_β and determine the potential Ψ_β. The IHP is separated from the OHP by a region of constant capacity C_2. The potential at the OHP is Ψ_d and an outer diffuse layer with charge σ_d neutralises the overall charge $(\sigma_0 + \sigma_d)$. The shear plane, where the zeta potential is assumed equivalent to Ψ_d, represents the frontier between the structured water near the oxide surface and the free water.

Reactions relatives to the amphoteric surface hydroxyls groups, which are uniformly distributed over the oxide planar surface, with respective thermodynamic equilibrium constant used to describe the system are:

(a) the protolysis reactions

$$\begin{aligned} &AlOH + H^+_{(aq)} \Longleftrightarrow AlOH_2^+ \\ &K^+ = [AlOH_2^+]/[AlOH][H^+]^* \exp(F\Psi_0/RT) \end{aligned} \quad (2)$$

$$\begin{aligned} &AlOH \Longleftrightarrow AlO^- + H^+_{(aq)} \\ &K^- = [AlO^-][H^+]/[AlOH]^* \exp(-F\Psi_0/RT) \end{aligned} \quad (3)$$

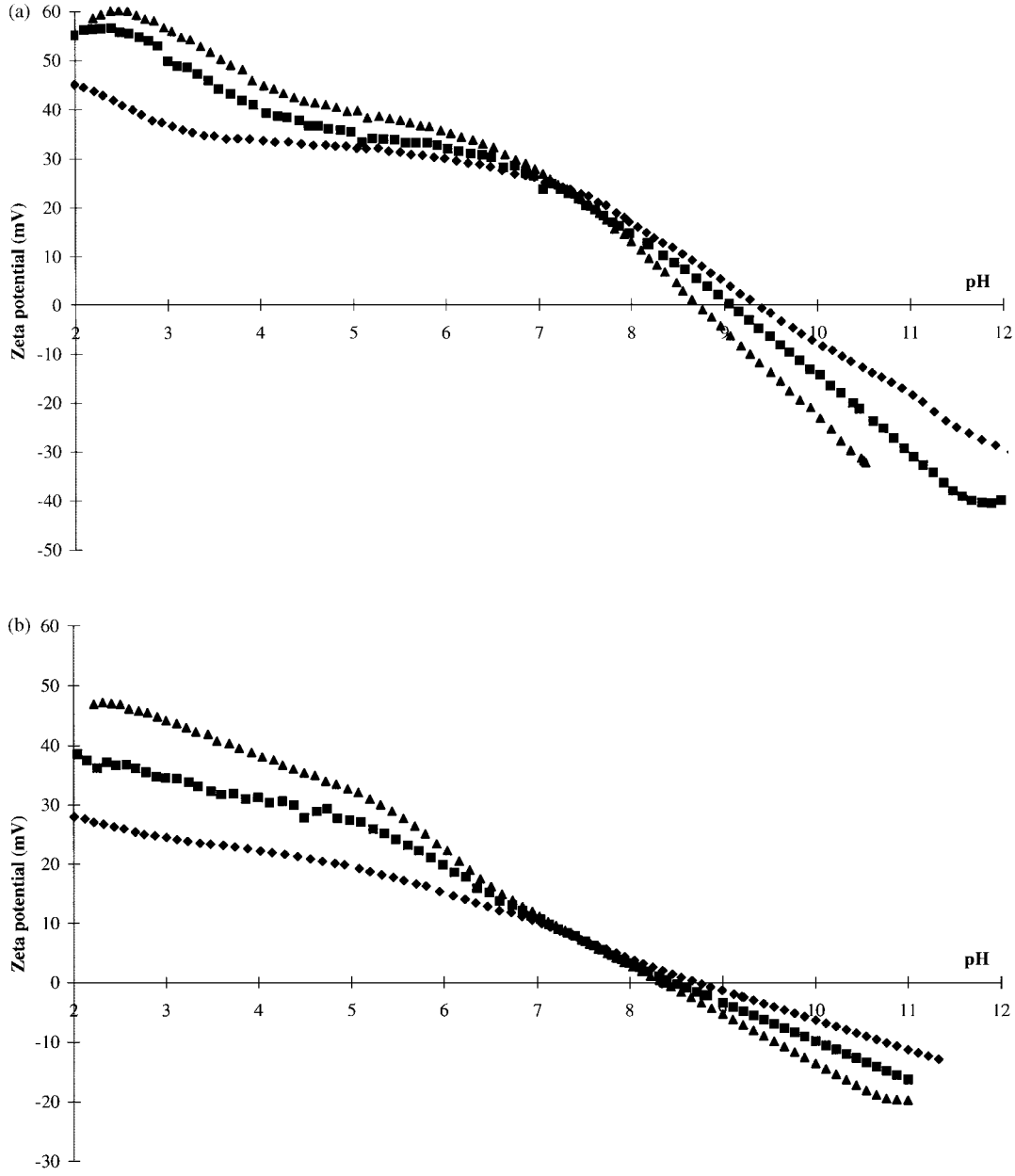

Fig. 3. Zeta potential data versus pH for (a) an AKP30 alumina suspension and (b) an A16SG at (◆) 10°C, (■) 20°C and (▲) 40°C (ionic strength fixed at 10^{-2} mol l^{-1}).

$$\begin{aligned} &H_2O \Longleftrightarrow H^+_{(aq)} + OH^-_{(aq)} \\ &Kw = [H^+](\gamma_{H+})[OH^-](\gamma_{OH-}) \end{aligned} \quad (4)$$

The activity coefficients γ_{H+} and γ_{OH-} are calculated according to the Davies equation and the TLM is applicable to systems ranging from near zero to ionic strengths up to 0·1 M, the upper limit of applicability of the Davies equation.[16]

(b) the electrolyte surface reactions

$$\begin{aligned} &AlOH + Na^+_{(aq)} \Longleftrightarrow AlO^-\text{-}Na^+ + H^+_{(aq)} \\ &K_{Na+} = [AlO^-\text{-}Na^+][H^+]/[AlOH][Na^+]^* \\ &\exp(F(\Psi\beta - \Psi_0)/RT) \\ &AlOH + Cl^-_{(aq)} + H^+_{(aq)} \Longleftrightarrow AlOH^+_2 - Cl^- \\ &K_{Cl-} = [AlOH^+_2 - Cl^-]/[AlOH][H^+][Cl^-]^* \\ &\exp(F(\Psi_0 - \Psi\beta)/RT) \end{aligned} \quad (5)$$

The total concentration of surface sites N_t is an estimation of the total number of exchangeable hydrogen atoms on the alumina surface. The value of N_t (mol l^{-1}) is related to the sites density N_s (sites nm^{-2}) through:

$$N_t = N_s SaC10^{18}/N_A \quad (7)$$

where Sa is the specific surface area (10 $m^2\,g^{-1}$), C the concentration of alumina in the suspension (136 g l^{-1}) and N_A, the Avogadro's number. Charge balance requires that the sum of the charges at the 0–, β– and d– planes be equal to

Table 2. Electrokinetic properties of (a) an aqueous alumina AKP30 suspension and (b) an aqueous alumina A16SG suspension.

Temperature (°C)	*Starting pH*	*ZPC*	*Zeta potential at pH=6 (mV)*	*Zeta potential at pH=8 (mV)*	*Zeta potential at pH=10 (mV)*
(a)					
10	8.5	9.3	30	16	−9
20	8	9.0	32	13	−14
40	7.65	8.85	35	12	−21
(b)					
10	9.2	8.7	16	3	−7
20	8.8	8.45	20	3	−10
40	8.37	8.35	22	3	−13

zero and the relationships between the charge and the potential are the following:

$$\sigma_d = -(8\varepsilon kTN_A I)^{1/2}\sinh(F\Psi_d/2RT) \qquad (8)$$

where I is the ionic strength.

$$\sigma_0 = (\Psi_0 - \Psi_\beta)C_1 \qquad (9)$$

$$\sigma_0 + \sigma_\beta = (\Psi_\beta - \Psi_d)C_2 = -\sigma_d \qquad (10)$$

and the surface charge ($C\,m^{-2}$) and mass balance equations relatives to this system are:

$$\sigma_0 = F/CSa([AlOH_2^+] + [AlOH_2^+ - Cl^-] - [AlO^-] - [AlO^- - Na^+]) \qquad (11)$$

$$\sigma_\beta = F/CSa([AlO^- - Na^+] - [AlOH_2^+ - Cl^-] \qquad (12)$$

$$N_t = [AlOH] + [AlOH_2^+] + [AlO^-] + [AlOH_2^+ - Cl^-] + [AlO^- - Na^+] \qquad (13)$$

This model requires seven adjustable fitting parameters including the two surface protolysis constants K^+ and K^- [eqns (2) and (3)], the two electrolyte surface binding constants K_{Cl-} and K_{Na+} [eqns (5) and (6)], the total site concentration N_t (eqn (13)) and the two capacitance parameters C_1 and C_2 [eqns (9) and (10)].

4.3.1.2. The potentiometric data fitting software FITEQL. In this study, the non linear least squares fitting program FITEQL 3·2[10] was used to find optimum model parameters values. This program optimises the values of adjustable parameters by changing their value until the sum of the squares of the residuals between the data and the calculate values is minimised. This computer program did not allow to fit directly the experimental zeta potential data and we were obliged to use titration data, (i.e. the total concentration of acid or base added versus pH) to get the values of adjustable parameters. Using these calculated values, theoretical curves were compared to the experimental data. The model incorporates the effect of background electrolyte concentration on titration behavior directly in model calculations. Unfortunately, the temperature is fixed at 298 K in the algorithm and can not be changed, then only data measured at 20°C were fitted. In order to compare the values of the adjustable parameters, additional data were recorded at an ionic strength fixed at 0·05 mol l^{-1} because ionic strength strongly influences the zeta potential values (Fig. 4). For a concentration of NaCl equal to 0·05 mol l^{-1}, the zero point charge did not change anymore (0·05 unit of pH); this electrolyte is neutral around the ZPC but the absolute value of zeta potential decreases (Table 3). The diffuse electrical double layer around each particle is compressed by the ions and the repulsive potential is reduced.

4.3.1.3. Procedure and results of the fits. Previous works[10] showed there are often many combinations of the variables that can give good fits to a set of titration data but in our study the combination of the parameters should fit zeta potential data too, then the number of combinations became restricted. Because of the large number of adjustable parameters, several should be fixed to get reasonable values and in general, the algorithm convergence occurs when fitting data using only two adjustable parameters. In the algorithm, among the seven adjustable parameters, K^+, K^-, K_{Cl-}, K_{Na+} and N_t can be fitted and the values of the capacitances C_1 and C_2 are fixed during the calculation.

The outer layer capacitance C_2 was always set to the typical value of 0·2 F m^{-2} and the value of the inner layer capacitance C_1 was included in the range 0·5 to 2 F m^{-1}. Steps of 0·1 F m^{-1} were used and the value of C_1 which leads to the best fit was kept.

Several experimental methods are used to determine Ns for oxides. In recent studies[16] tritium

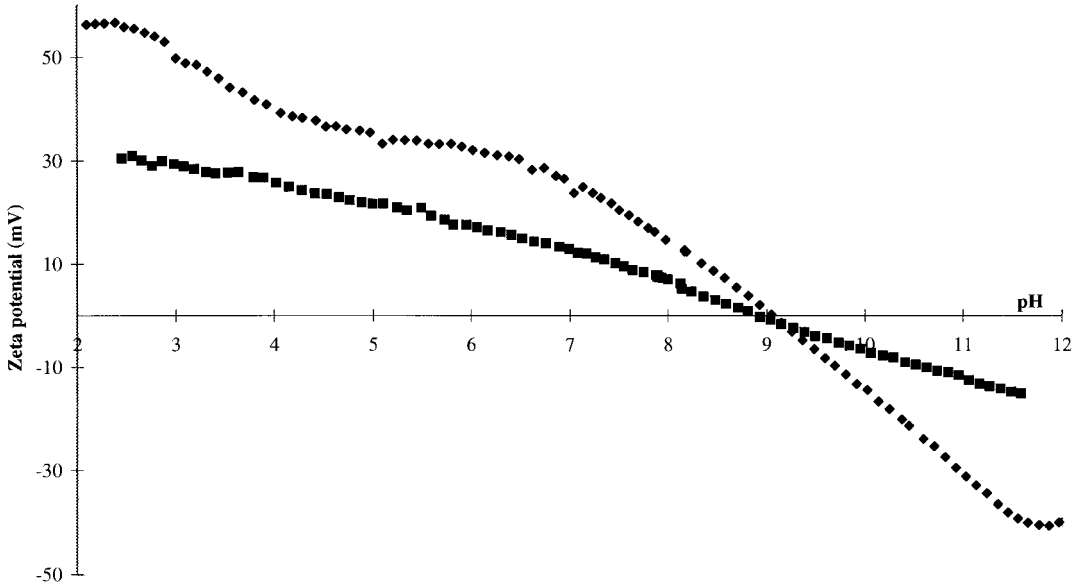

Fig. 4. Zeta potential data versus pH for an AKP30 alumina suspension at 20°C for a ionic strength of (◆) 10^{-2} mol l^{-1} and (■) 510^{-2} mol l^{-1}.

Table 3. Electrokinetic properties of AKP30 suspensions at two ionic strengths

Ionic strength (mol l^{-1})	*ZPC*	*Zeta potential at pH 10 (mV)*	*Zeta potential at pH 7 (mV)*
0·01	8·95	−18	−28
0·05	8·9	−8	−17

exchange is considered to be the best experimental estimate for Ns and this method gives a larger value than these obtained by acid base titration (i.e. 2 sites nm^{-2}). Potentiometric acid base titration may underestimate site density because accumulation of surface charge may prevent from complete ionisation. For our calculations, a minimum value of 10 sites nm^{-2} was retained.

Concerning the proton equilibrium constant, this following constraint was used:

$$\mathrm{ZPC} = (\log \mathrm{K}^{+} - \log \mathrm{K}^{-})/2 \qquad (14)$$

considering that the number of ionised sites at the ZPC is very low and ΔpKa is greater than 2. A theoretical prediction[17] of single site surface protonation equilibrium constants for oxide in water based on the Born solvation theory gives for alumina a value of 5 for ΔpKa. Then, we have chosen to test the two values 4 and 5. The procedure of the fit was the following: for a given value of ΔpKa of 4 or 5, ($K^{+} = \mathrm{ZPC}\text{-}\Delta pKa/2$ and $\mathrm{K}^{-} = \mathrm{ZPC} + \Delta pKa/2$), calculations were carried out until finding reasonable values of C_1 and N_t which fit in the best way the experimental data. The electrolyte binding constants are taken from the result of the fit.

Table 4 summarizes the combinations of values of N_s, C_1, $K_{\mathrm{Cl}-}$ and $K_{\mathrm{Na}+}$ which give the best fit for both titration and zeta potential data in function of pH from 5 to 11 for a given ΔpKa. Experimental data and theoretical curves using these values are compared in Fig. 5.

The values of V which is an indicator of the goodness of the fit are higher than those given (< 20) by the authors of FITEQL to consider a reasonably good fit. Indeed figures show that the calculated curves are far from the experimental data in particular for acid pH but the calculated zeta potential values fit better the experimental data and this is the aim of this study. For the same ionic strength, the value of 5 for ΔpKa leads to a higher value of C_1 and V but the calculated zeta potential values are nearly identical to those obtained for $\Delta pKa = 4$. The values of the electrolyte constants do not vary anymore whatever the ionic strength, and the values of pKa are similar to those obtained in previous works.[16] The ionic strength of 0·05 mol l^{-1} leads to a higher density of surface sites which can be due to the better screen effect of the surface charge by specifically adsorbed ions from electrolyte.

As a combination of reasonable values of the adjustable parameters allows the fit of zeta potential data, the interpretation of the evolution of the curve at 20°C for the AKP30 alumina was based on the TLM. From the ZPC to pH 7, which corresponds to the beginning of the plateau, the linear variation of zeta potential is governed by the reaction of hydroxyl groups protonation and the formation of the ion pairs with the chloride ions. The plateau, which is observed at pH 7 with a zeta potential of 25 mV indicates ionisation of a large

number of available hydroxyl surface groups. The deprotonation of an identical number of surface groups should lead to a plateau at basic pH but for pH > ZPC, the deprotonation of hydroxyl groups occurs and sodium pairs are formed. From the value of −25 mV measured at the pH of 10·3, the potential continues to decrease strongly and the model fit no longer experimental data. This suggests that another phenomena should contribute to increase the negative surface charge, maybe the solubility of alumina. Evanko *et al.*[18] showed that alumina is stable at 20°C in the range of pH from 5 to 10 at 20°C. The same tendency is observed for acidic pH lower than pH 5 where the model can not account for the increase of the potential after the plateau.

Table 4. Results of fits

Ionic strength ($mol\,l^{-1}$)	ΔpKa	K^+	K^-	N_s ($sites\,nm^{-2}$)	C_1 ($F m^{-1}$)	K_{Cl-}	K_{Na+}	V
0·01	4	6·95	10·95	10	1	8·4	9·1	150
0·01	5	6·95	10·95	10	1·2	8·2	9·2	240
0·05	4	6·9	10·9	14	1·2	8·5	8·9	285
0·05	5	6·9	10·9	14	1·4	8·3	9·0	374

4.3.2 *Effect of the temperature*

Considering the curves obtained at 10 and 40°C [Fig. 3(a)], the temperature has a strong effect on the variations of zeta potential versus pH. In the

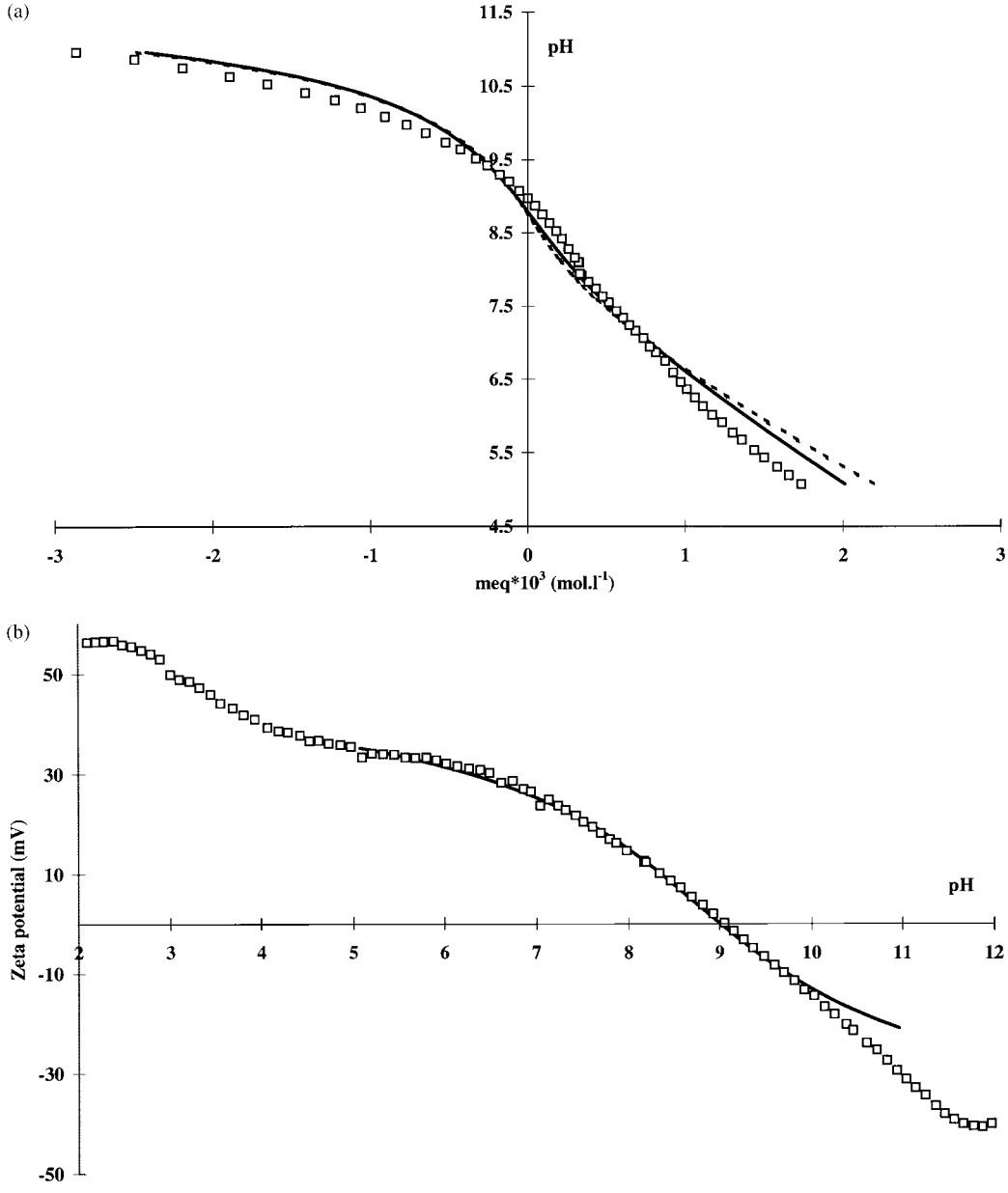

Fig. 5. (a) Fit of titration data at an ionic strength of 0·01 mol l^{-1}: (—) $\Delta pKa = 4$; (- - -) $\Delta pKa = 5$; (□) experimental data. (b) Fit of zeta potential data at an ionic strength of 0·01 mol l^{-1}: $\Delta pKa = 4$ or 5, calculated curves are superimposed; (□) experimental data.

(continued on next page)

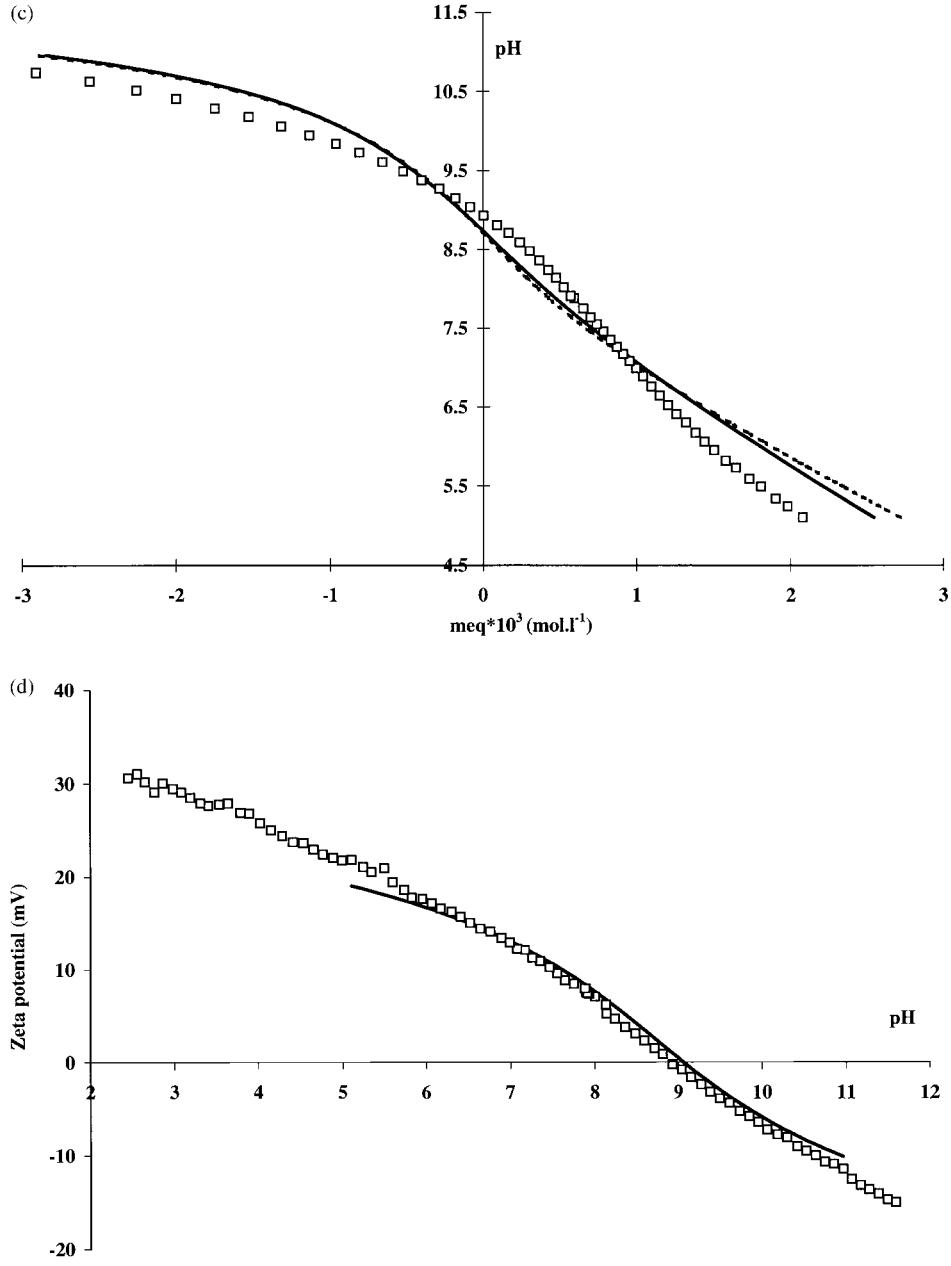

Fig. 5. *(continued)* (c) Fit of titration data at an ionic strength of 0·05 mol l^{-1}: (—) $\Delta pKa = 4$; (- - -) $\Delta pKa = 5$; (□) experimental data. (d) Fit of zeta potential data at an ionic strength of 0·05 mol l^{-1}: $\Delta pKa = 4$ or 5, calculated curves are superimposed; (□) experimental data.

range of pH 7–11, the slope of the linear part increases with the temperature. The increase of the potential at acidic pH starts at a more basic pH at high temperature (i.e. 5 at 40°C, 4·2 at 20°C and 3 at 10°C) then the length of the plateau is reduced. The ZPC and the starting pH shift to acidic values from 10–40°C and excluding the pH range 7–9·2 (ZPC at 10°C), the absolute values of the zeta potential are slightly higher at high temperature.

As the computer program can not integrate variations of temperature, only some hypothesis from results obtained at 20°C can only be done. The variation of ZPC leads to a decrease of K^+ and K^- at 40°C and an increase of the two constants at 10°C if ΔpKa remains constant. The variations of zeta potential corresponding to the linear part ($7 < pH < 11$) which are faster at 40°C indicate that the protonation and deprotonation of the hydroxyl groups are activated by the temperature. Concerning the specific adsorption of electrolyte ions, NaCl is neutral around the ZPC but for high potentials either negative or positive, the corresponding counter ion should be preferentially adsorbed. As temperature affects the amplitude of the zeta potential, a large number of ion pairs especially AlO^-Na+ are formed for basic pH at 40°C and then equilibrium constants should be affected by the temperature. At pH 5.5 which corresponds approximately to the middle of the plateau, there is a small difference of 7 mV between the higher (40°C) and the lower (10°C) value of zeta potential, then the number of sites should remain almost constant whatever the temperature.

On the other hand, an increase of temperature should reduce the pH range of the alumina stability and the contribution of the solubility of the oxide to the positive surface charge at acidic pH may likely explain the diminution of the length of the plateau at high temperature.

Finally, the shear plane where the zeta potential is measured and which characterises the limit between the structured water near the surface and the free water should move with variations of the temperature. The layer of physically adsorbed water is likely thinner at 40°C than at 20°C and the shear plane approached the surface of particules, leading to a higher zeta potential value. At 10°C the shear plane moves away from the surface and smaller values of zeta potential were measured.

Concerning the A16SG powder, the same analysis can be made. As a function of pH and of temperature, the zeta potential varies in the same way for the AKP30 powder. Because of the decomposition of the impurities in water, in particular Na_2O (0·06 wt%), the surface charge at the starting pH is negative and the ZPC smaller than 9 which leads to a more acidic surface for this powder in water. At given pH and temperature, the absolute values of zeta potential of A16SG are lower than those of high purity AKP30 (Table 2). This suggests that the number of available hydroxyl groups was lower. Measurements of active sites by isotopic exchange should be made to confirm this hypothesis.

4.4 With Dispersant

4.4.1 With Tiron dispersant

The two alumina powders were used to study the effect of Tiron (0·2 wt%) on the stability of the slurries at 10, 20 and 40°C. Results are reported in Fig. 6 and in Table 5(a) and (b). The curves represent the evolution of the zeta potential versus pH from the starting pH to pH 2.

4.4.1.1. Effect of pH at 20°C. When Tiron is added, the anion adsorbs onto the surface of alumina and produces a high density of negative surface charge. Whatever the powder, each curve can be described by two steps almost linear. First from the starting pH, for which the negative surface charge is the highest, the absolute value of zeta potential decreases linearly and slowly down to pH of about 5. Then, the decrease becomes more abrupt for acidic pH to reach the ZPC. As without dispersant, smaller absolute values of zeta potential were measured with the A16SG powder. The ZPC was reached for a pH equal to 3.5 and 3 for A16SG and AKP30 powders respectively.

The computer program FITEQL had not been used to fit these data because the equilibrium constant corresponding to the coordination complexe between the hydroxyl surface groups and the Tiron is not known. The ligand exchange model describes the adsorption of the Tiron as an exchange between the anion and a hydroxyl surface group. In the case of a concentration of 10 sites nm^{-2}, a large number of hydroxyl groups remains available. At the starting pH of about 9, the surface groups are neutral but as soon as the pH become more acidic, their protonation should occur and constitute a positive contribution to the total surface charge which should compensate the negative charge due to the Tiron at the ZPC. In the case of this hypothesis, the protonation does not occur in the same way as without Tiron because the beginning of the rapid decrease of the negative surface charge between pH 5.5 and 6 corresponds approximately to the middle of the plateau observed on the previous curves (without dispersant, Fig. 3) and vice versa between pH 9 and 5.

No adsorption isotherm of Tiron has been established onto the AKP30 powder, but the quantity of Tiron adsorbed is likely larger than the amount adsorbed onto the A16SG powder. These results can confirm the previous hypothesis concerning the number of hydroxyl surface groups and justify the smaller zeta potential values measured with the A16SG powder.

4.4.1.2. Effect of the temperature. The slope of the two linear parts increase with the temperature and at the starting pH, a temperature of 40°C leads to the highest zeta potential value (Table 5). The difference, between potentials observed at each temperature is more pronounced for the AKP30 powder. This difference reduced as soon as the pH decreased to reach the same ZPC for the three temperatures tested. The lowest starting value of zeta potential measured at 10°C is compensated by a slower variation of zeta potential with pH.

Adsorption isotherms established with the A16SG powder showed that the quantity of Tiron adsorbed did not vary with temperature and we can consider that this result can be transposed to the AKP30 powder. Then the negative contribution to the surface charge due to the adsorbed Tiron remains constant at each pH whatever the temperature. The variation of the total surface charge versus pH should only depend of the positive contribution due to the protonation of the free hydroxyl groups. In the previous study, we concluded that the temperature activates the protonation of the OH groups; onto the surface of particles in presence of the dispersant, the temperature seems to produce the same effect. The decrease of the absolute value of the zeta potential is faster at 40°C than at 10°C. As the quantity of Tiron adsorbed did not vary with temperature, the high

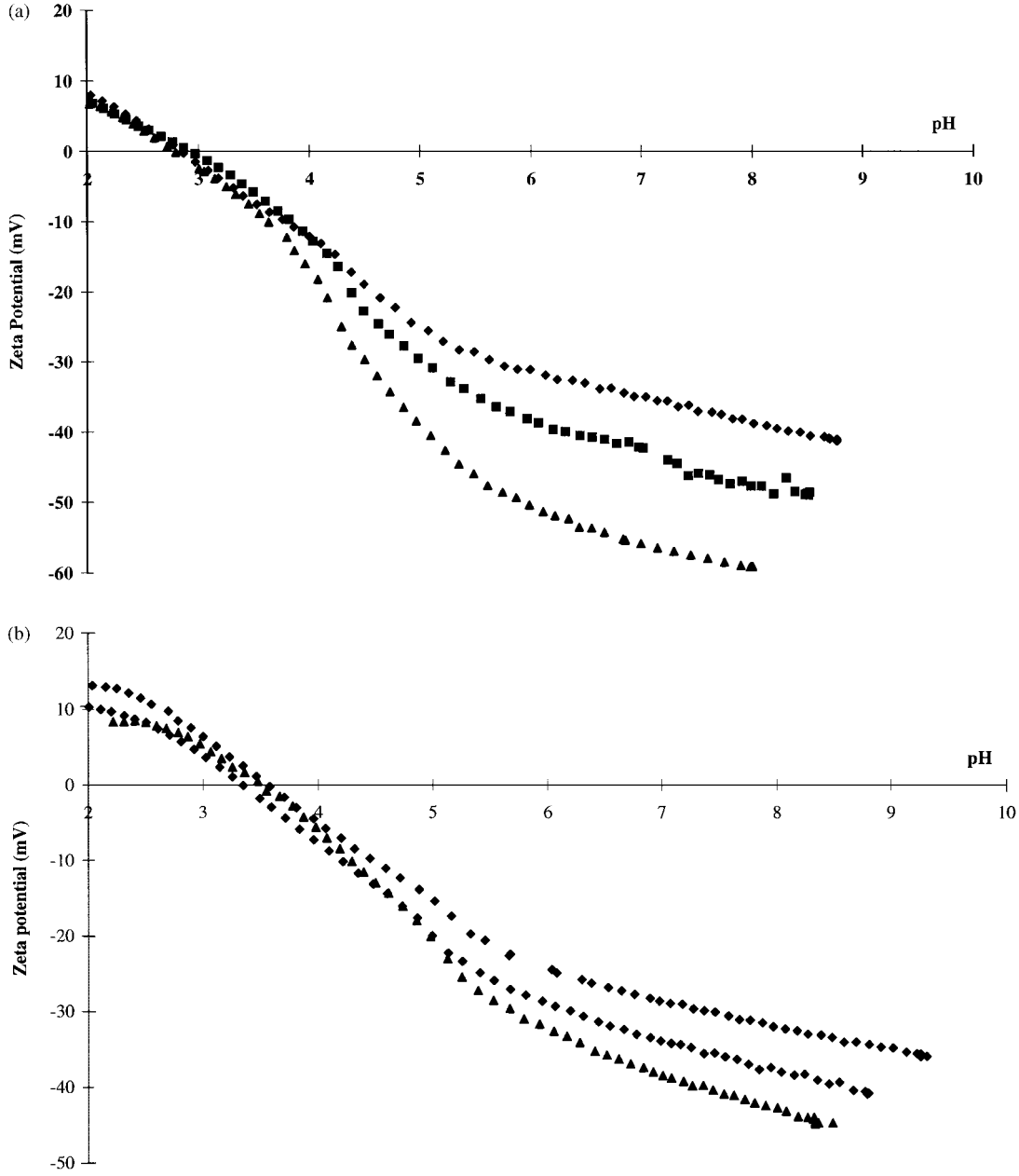

Fig. 6. Zeta potential data versus pH for (a) an AKP30 and (b) an A16SG alumina suspension with 0·2 wt% of Tiron at (◆) 10°C; (■) 20°C; (▲) 40°C (ionic strength fixed at 10^{-2} mol l^{-1}).

Table 5. Electrokinetic properties of (a) AKP30 and (b) A16SG suspensions with Tiron at 10, 20 and 40°C

Temperature (°C)	*ZPC*	*Zeta potential at pH 8 (mV)*	*Zeta potential at pH 5 (mV)*
(a)			
10	3	−38	−26
20	3	−47	−30
40	3	−60	−40
(b)			
10	3·5	−31	−16
20	3·5	−37	−20
40	3·5	−42	−20

zeta potential value at pH 8 and at 40°C suggests, as for the previous system, that the shear plane approaches the particle surface.

4.4.2 With PMAANa dispersant

Measurements with the polyelectrolyte versus temperature were carried out only with the A16SG powder and the results are shown in Fig. 7. At a given temperature, as for the Tiron, the negative surface charge developed by the ionisation of the carboxylate groups decreases when the pH becomes more acidic first slowly and more faster from pH 5·5. The ZPC is reached for a pH of 4·3 whatever the temperature, curves are similar and small differences of zeta potential values are observed between each temperature for a given pH. At pH 8, these values are in the same order as those measured with Tiron, the higher value of ZPC could be explained by the neutralization of the carboxylate functions ($\Delta pKa = 6$, Fig. 1) with

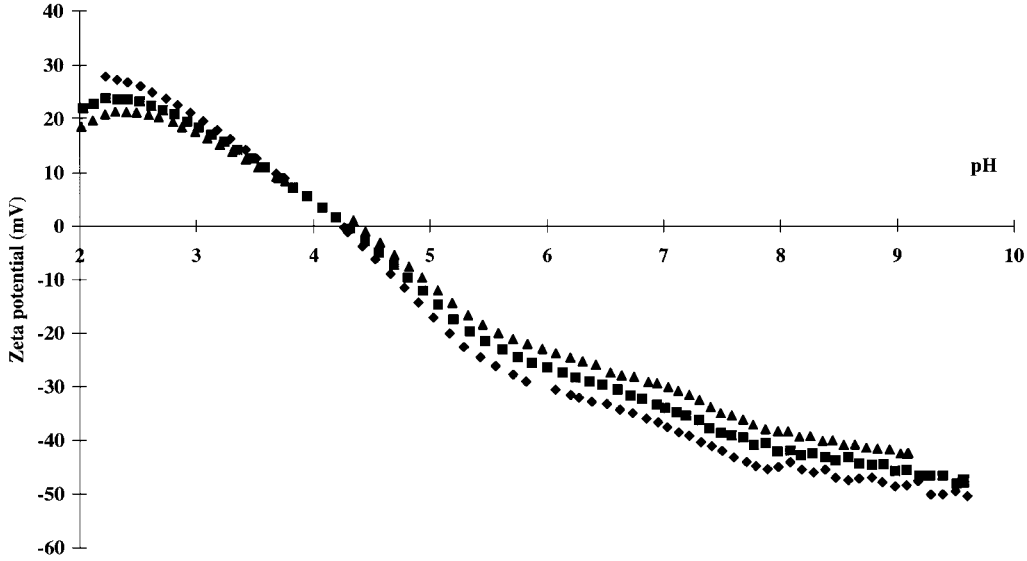

Fig. 7. Zeta potential data versus pH for an A16SG alumina suspension with 0·3 wt% of PMAANa at (◆) 10°C; (■) 20°C; (▲) 40°C (ionic strength fixed at 10^{-2} mol l^{-1}).

the addition of acid which leads to a decrease of the negative contribution of the surface charge.

The mechanism of particle dispersion using this type of polyelectrolyte is based on both electrostatic repulsion and steric stabilisation. With an average molecular weight of 9500, the gyration radius of PMAANa under unconstrained conditions can be estimated about 6 nm and for an ionic strength of 10^{-2} mol l^{-1}, the thickness of the diffuse electrical double layer is evaluated at 3 nm.[19] Because of the steric effect due to the polymer, the shear plane is not able to move in regards to the surface with the variation of the temperature which should lead to nearly identical curves of zeta potential.

5 Conclusion

A strong adsorption of dispersant onto alumina surface is not affected by the variation of the temperature but a temperature higher than 40°C strongly influences the amplitude of the repulsive potential created between the particles, in particular when the Tiron is used as dispersant. The shear plane where the zeta potential is measured should approache the surface of particles covered by the anionic dispersant leading to a higher potential and because of the steric effect due to the polymer, the shear plane is not able to move in regards to the surface with the variation of the temperature leading to the same potential at a given pH. Further measurements of viscosity show that the increase of the temperature leads to a decrease of the apparent viscosity of concentrated suspensions (80 wt% of A16SG alumina) whatever the dispersant used.

At 60°C and at pH 9, the pH of very concentrated alumina slurries prepared with Tiron, the higher zeta potential value measured corresponds to the smaller value of viscosity but several parameters with different temperature dependence should influence the rheological behaviour of such suspensions and a rigorous interpretation can be done only with complementary study. Then, this work shows that the temperature is beneficial to improve the stability of alumina slurries and permits to concentrate it.

Acknowledgements

This work was supported by the European Commission CEC Human Capital and Mobility Programme, Contract CHRX-CT94-0574, 'Application of fundamental principles of colloid and interface science and rheology to ceramic forming processes.'

References

1. Wen-Cheng, J., Wei, Su Jen Lu and Bu-Kon, Yu, Characterization of submicron alumina dispersions with polymethacrylic acid polyelectrolyte. *J. Eur. Ceram. Soc.*, 1995, **15**, 155–164.
2. Greenwood, R. and Bergström, L., Electroacoustic and rheological properties of aqueous Ce–ZrO_2 suspensions. *J. Eur. Ceram. Soc.*, 1997, **17**, 537–548.
3. Vermeer, A. W. P., Leermakers, F. A. M. and Koopal, L. K., Adsorption of weak polyelectrolytes on surfaces with a variable charge. Self-consistent-field calculations. *Langmuir*, 1997, **13**, 4413–4421.
4. Linse, P., Adsorption of weakly charged polyelectrolytes at oppositely charged surfaces. *Macromolecules*, 1996, **29**, 326–336.
5. Cesarano, J. and Aksay, I. A., Processing of highly concentrated aqueous α-alumina suspensions stabilized with

polyelectrolytes. *J. Am. Ceram. Soc.*, 1988, **71**(12), 1062–1067.
6. Baklouti, S., Pagnoux, C., Chartier, T. and Baumard, J. F., Processing of aqueous α-Al_2O_3, α-$SiO_2$$\alpha$-SiC suspensions with polyelectrolytes. *J. Eur. Ceram. Soc.*, 1997, **17**, 1387–1392.
7. Baader, F. H., Graule, T. J. and Gauckler, L. J., Direct coagulation casting. A new green shape technique part II: Application to alumina. *Ind. Ceram.*, 1996, **16**, 1.
8. Hidber, P. C., Graule, T. J. and Gauckler, L. J., Influence of the dispersant structure on properties of electrostatically stabilized aqueous alumina suspensions. *J. Eur. Ceram. Soc.*, 1997, **17**, 239–249.
9. Tomita, Y., Guo, L., Zhang, Y., Uchida, N. and Uematsu, K., Effect of temperature on the slurry characteristics and green bodies of alumina. *J. Am. Ceram. Soc.*, 1995, **78**(8), 2153–2156.
10. Herbelin, A. L. and Westall J. C., FITEQL 3.2, a computer program for determination of chemical equilibrium constants from experimental data, Department of Chemistry, Oregon State University, Corvallis, OR, 1996.
11. Cesarano, J. and Aksay, I. A., Stability of aqueous α-alumina suspensions with polymethacrylic acid polyelectrolyte. *J. Am. Ceram. Soc.*, 1988, **71**(4), 250–255.
12. Pagnoux, C., Chartier, T., Granja, M. De F., Doreau, F., Ferreira, J. M. and Baumard, J. F., Aqueous suspensions for tape-casting based on acrylic binders. *J. Eur. Ceram. Soc.*, 1998, **18**, 241–247.
13. O'Brien, R. W., Electroacoustic effects in a dilute suspension of spherical particles. *J. Fluid. Mech.*, 1988, **190**, 71–86.
14. Stumm, W., Kummert, R. and Sigg, L., A ligand exchange model for the adsorption of inorganic and organic ligands at hydrous oxide interfaces. *Croat. Chem. Acta*, 1980, **53**(2), 291–312.
15. Sahai, N. and Sverjensky, D. A., Evaluation of internally consistent parameters for the triple-layer model by the systematic analysis of oxide surface titration data. *Geochim. Cosmochim. Acta*, 1997, **61**(14), 2801–2826.
16. Hayes, K. F., Redden, G., Ela, W. and Leckie, J. O., Surface complexation models: An evaluation of model parameter estimation using FITEQL and oxide mineral titration data. *J. Colloid Interface Sci.*, 1991, **142**(2), 448–469.
17. Sverjensky, D. A. and Sahai, N., Theoretical prediction of single-site surface-protonation equilibrium constants for oxides and silicates in water. *Geochim. Cosmochim. Acta*, 1996, **60**(20), 3773–3797.
18. Evanko, C. R., Delisio, R. F., Dzombak, D. A. and Novak, J. W., Influence of aqueous solution chemistry on the surface charge, viscosity and stability of concentrated alumina dispersions in water. *Colloids and Surfaces A*, 1997, **125**, 95–107.
19. Zupancic, A., Lapasin, R. and Kristofferson, A., Influence of particle concentration on rheological properties of aqueous αAl_2O_3 suspensions. *J. Eur. Ceram. Soc.*, 1998, **18**, 467–477.